Dražen Kustura
Frane Vlak ✉
Tomislav Matić
Marko Vukasović

https://doi.org/10.21278/TOF.473053623
ISSN 1333-1124
eISSN 1849-1391

THE OUT-OF-PLANE STATIC ANALYSIS OF THIN-WALLED CURVED H-BEAMS

Summary

This paper presents an approximate approach to the out-of-plane linear static analysis of isotropic thin-walled curved beams with doubly symmetric H-shaped cross-sections, whose undeformed centroid line is the circular arc. The governing equations are derived using Vlasov's assumptions, the elasticity equations expressed in the cylindrical coordinate system, and the equilibrium equations for the curved centroid line. The terms containing the curvature effect are linearized by neglecting the higher order terms of the Maclaurin series expansion. With this linearization, the geometric properties for straight thin-walled beams can be used. An additional simplification is introduced by using the warping moment−bimoment relation for straight thin-walled beams. The approximate closed-form solutions for long, slightly, and moderately curved beams, obtained by the proposed and Vlasov's approaches, are compared with the results of the shell finite element analysis by investigating the influence of beam length and curvature on displacements and normal stress.

Key words: *thin-walled curved beam, doubly symmetric H cross-sections, out-of-plane static analysis, closed-form solutions.*

1. Introduction

The curved beams with thin-walled open cross-section find numerous applications in various engineering fields (curved parts of highways, public and industrial buildings, and ship and offshore structural elements, for example) due to their attractiveness and favorable stiffness-to-mass ratio. Due to the existence of initial curvature and the complex internal force−displacement relations with coupling effects of the internal forces, the structural analysis of curved beams is more complicated than that of the straight beams. For doubly symmetric cross-sections, commonly used for curved girders, the axial force (the circumferential force) and the in-plane bending moment (moment about the principal axis perpendicular to the plane of curvature) are coupled, as are the torsional moment and the out-of-plane bending moment (moment about the principal axis in the plane of curvature moment). For asymmetric cross-sections, all internal forces are coupled, while in the case of monosymmetric cross-sections, the coupling effects depend on the shape of the cross-section [1].

Vlasov [2] proposed governing equations for thin-walled curved beams with an arbitrary, open cross-section shape, where undeformed centroid line is curved into a circular arc. To obtain the internal force−displacement relations of curved thin-walled beams with small curvature, Vlasov replaced the strain measures of straight beams with those of curved beams in the internal force−displacement relations of straight beams. The governing equations were obtained using the free-body approach, neglecting the distances between the shear centre and the cross-section centroid in the equilibrium equations. In his approach, Vlasov assumed that the cross-sectional distortion and the shear strain in the middle surface can be neglected. Timoshenko [3] used the same approach in the in-plane analysis of curved beams, where warping is neglected, but he additionally assumed that the centroid line is inextensible. Yoo used a similar approach in his study [4]. It must be emphasized that the majority of papers published in the last 30-40 years, that are related to the analytical solutions for the curved beams, deal with buckling and vibration problems. The papers that are important for this research, [1, 5-11], are based on previously mentioned Vlasov's assumptions; they are presented in more detail in the following paragraph.

Nishino and Fukusawa [5] performed a linear analysis of thin-walled curved beams by setting the expression for the longitudinal displacement that was subsequently used in other studies [6-8]. Usami and Koh [6] introduced an infinitesimally thin fictitious thin-walled branch to obtain the longitudinal centroid displacement. The linear parts of the Maclaurin series expansion for terms containing the curvature effect in the longitudinal displacement expression are used in [7], while the quadratic terms of series expansion are used in [8]. Yang and Kuo [9-11] performed the analysis of thin-walled curved beams by neglecting the membrane component of shear stress, as stated in [12]. A modified expression for the longitudinal displacement is proposed in [9], the influence of radial stresses on curved beams is investigated in [10], while the curved beam finite element is introduced in [11].

To the best of the authors' knowledge, Tong and Xu [1] were the first to extend Vlasov's approach using the elasticity equations for shells of revolution [13]. In their study, Tong and Xu, [1], presented a detailed comparison between their approach, Vlasov's approach, and other approaches [6, 9] based on Vlasov's assumptions. According to the approaches presented in [1] and [9], and contrary to the approaches presented in [5-8], the longitudinal displacement expression for a doubly symmetric I-shaped cross-section differs from that for a doubly symmetric H-shaped cross-section, where an additional term, related to the cross-sectional warping, exists.

The aforementioned methods are still used in the analysis of curved beams. For example, the analyses of ring beams in [14] and [15] are based on Vlasov's approach, while the analysis of thin-walled curved composite beams in [16] is based on the approach of Tong and Xu. Kustura et al. [17] presented a simplification of the approach for calculating the longitudinal displacement given in [9] by obtaining closed-form solutions required for the in-plane static analysis of thin-walled curved beams with doubly symmetric I- and H-shaped cross-sections.

Numerical methods dealing with the static and buckling responses of thin-walled structures [18], particularly with the curved beams, are developed and studied to a larger extent than analytical methods. Beam finite elements are used for the analysis of curved beams [19] and thin-walled curved beams [8, 20-22]. The influence of shear is neglected in [8, 20] while it is considered in [21, 22]. The isogeometric finite element analysis of complex thin-walled structures [23] is also used for the analysis of the curved [24, 25] and curvilinear beams [26, 27]. Generalised beam theory is implemented in the analysis of thin-walled beams with cross-sections having two axes of symmetry [28, 29] and one axis of symmetry [28, 30]. Carrera's unified formulation for straight thin-walled beams [31] is also applied in the analysis of curved beams [32].

Regarding the linear static analysis of curved thin-walled H-beams, it must be emphasized that none of the above-mentioned analytical studies provide solutions for displacements and stresses in closed form. It should be noted that all these analyses provide only the governing equations without giving their solutions in analytical form and mostly without specifying boundary conditions for different types of supports. Therefore, the main objective of this study is to provide closed-form solutions for the out-of-plane analysis of curved thin-walled beams with doubly symmetric H cross-sections.

In this paper, Vlasov's assumptions and the expression for longitudinal displacement of the H cross-section given in [1, 9] are used to determine the longitudinal strain and, consequently, the normal stress. Based on the normal stress, the internal forces−displacement relations are established. All the terms containing the curvature effect in these relations are consistently linearized using the Maclaurin series expansion in which higher order terms are neglected. This simplification is also used in [7], but in that study it is applied to different internal force−displacement relations since its definition is based on a different expression for longitudinal displacement. As a consequence of this simplification, in this study, all geometric properties for curved beams are replaced with straight thin-walled beam properties, in contrast to [1] where some of the geometric properties retained curvature terms. In addition, in-plane forces and displacements are decoupled from the out-of-plane components. Since the curvature effect is approximately considered with this linearization, the solutions obtained with this approach should be applicable to moderately and slightly curved beams. Moreover, instead of using the modified bimoment to define the curved beam warping moment [1], this study uses the relationship between the warping moment and the bimoment [2] that is valid for straight thin-walled beams. Thus, the warping moment is included in the calculation of the total torsional moment, while it is neglected in [9].

The second section of the paper deals with the procedure for deriving the governing equations based on the equilibrium equations of the free-body approach and the closed-form solutions for displacements obtained using the method of initial parameters. In the third section, the solutions obtained using the proposed approach and Vlasov's approach are compared with shell finite element solutions for different curvatures and beam lengths. As previously mentioned, the solutions of the governing equations in all references are not given in analytical form, which requires the use of different numerical procedures to solve systems of coupled differential equations. For this reason, only Vlasov's approach is used for the comparison and its solutions are presented in analytical closed form in Appendix B. Moreover, Vlasov's approach is chosen as the first systematically derived approach for the analysis of thin-walled beams; it is used in almost all references [1, 5-17, 20, 21, 24, 28-31, 33, 35, 36] for the same purpose. In contrast to [1], Vlasov used the geometric properties of straight thin-walled beams; the same is done in this paper. Finally, conclusions are drawn in the last section of the paper.

2. Theoretical development

2.1 Displacements and normal stress

The middle surface of a thin-walled curved beam with a doubly symmetric H-shaped cross-section is shown in Fig. 1, while the geometry of the cross-section is shown in Fig. 2. The undeformed centroid line of this curved beam is a circular arc with a radius R. In the following analysis, the cylindrical coordinate system O$\rho\phi Z$ and the curvilinear coordinate system Cxyz are used, where $\rho = R - y$ and $\phi = x/R$. The origin C is located at the cross-section centroid and the origin O is located at the centre of the undeformed curved centroid line. The positive direction of the x-axis corresponds to an increase in the angle, ϕ, while the

y- and *z*-axes are the principal axes of the cross-section; *u*, *v*, and *w* are displacements of any point S on the middle surface (Fig. 2) and u_C, v_C and w_C are displacements of the cross-section centroid C in the direction of the *x*-, *y*- and *z*-axes, respectively.

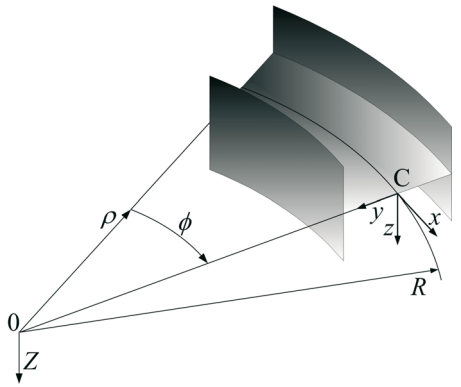

Fig. 1 Global and local coordinate systems

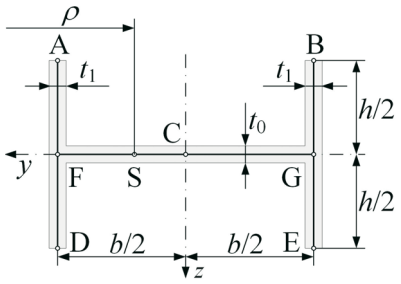

Fig. 2 H cross-section

The analysis presented in this study is limited to the out-of-plane static analysis of a doubly symmetric H-shaped cross-section with flanges perpendicular to the plane of curvature. The governing expressions presented in this paper are derived based on the following assumptions:

(1) the strains and displacements are small,

(2) the cross-section middle line is rigid in its own plane,

(3) the shear strain in the middle surface is neglected, and

(4) the material is linear elastic.

In order to present approximate closed-form solutions, the following constraints are introduced in this study:

(a) the initial curvature of the beam is moderate ($R/b^* > 7$, where b^* is the dimension of the largest cross-section wall), and

(b) only the uniformly distributed line loads are considered.

If the doubly symmetric cross-section rotates as a rigid body in its own plane, the transverse displacements for the point S are defined as follows [1, 2, 9]:

$$v = v_C - z\alpha, \qquad w = w_C + y\alpha, \tag{1}$$

where α is the angle of torsion (twist angle). Based on the strain−displacement relations presented in [7] and following the approach presented in [1, 9], where the shear strain in the middle surface is neglected, the expression for the longitudinal displacement *u* of a point S for a doubly symmetric H-shaped cross-section (Fig. 1) is defined as follows:

$$u = u_C - y\gamma + z\beta + \omega\vartheta\frac{R}{R-y}\ , \tag{2}$$

with

$$\gamma = v_C' + u_C/R, \qquad \beta = -w_C', \qquad \vartheta = -\left(\alpha' + w_C'/R\right), \tag{3}$$

where $\omega = y{\cdot}z$ is the sectorial coordinate, γ and β are the slopes of the deflection line in the C*xy* and C*xz* planes, respectively, ϑ is the relative angle of torsion [8], and $()' = \mathrm{d}()/\mathrm{d}x$. The last term on the right-hand side of Eq. (2) represents the warping displacement, where the term $R/(R - y)$ introduces the curvature effect.

The longitudinal strain ε_x for curved beams is defined as follows [7, 13]:

$$\varepsilon_x = \frac{R}{R-y}\left(\frac{\partial u}{\partial x} - \frac{v}{R}\right). \tag{4}$$

According to Hooke's law, the normal stress is $\sigma_x = E\varepsilon_x$, where E is the modulus of elasticity. For doubly symmetric H cross-sections, using Eqs. (1) – (4), one obtains [1, 9]

$$\sigma_x = E\left[u_\mathrm{C}' - \frac{v_\mathrm{C}}{R} - y\left(v_\mathrm{C}'' + \frac{u_\mathrm{C}'}{R}\right) - z\left(w_\mathrm{C}'' - \frac{\alpha}{R}\right) - \frac{\omega R}{R-y}\left(\alpha'' + \frac{w_\mathrm{C}''}{R}\right)\right]\frac{R}{R-y}. \tag{5}$$

2.2 Internal force – displacement relations

The internal force–normal stress relations for curved thin-walled beams are defined in the same way as for the straight ones [1, 2], i.e.,

$$N = \int_A \sigma_x \mathrm{d}A, \qquad M_z = -\int_A \sigma_x y \mathrm{d}A, \qquad M_y = \int_A \sigma_x z \mathrm{d}A, \qquad B = \int_A \sigma_x \omega \mathrm{d}A, \tag{6}$$

where N, M_z, M_y, and B are the longitudinal force, the bending moment about the z-axis, the bending moment about the y-axis, and the bimoment, respectively. When the full curvature effect is taken into account, the internal force–displacement relations are obtained on the basis of Eqs. (5) and (6), i.e.,

$$\begin{bmatrix} N \\ M_z \\ M_y \\ B \end{bmatrix} = E\left(\int_A \begin{bmatrix} 1 & -y & -z & -\omega\dfrac{R}{R-y} \\ -y & -y^2 & \omega & y\omega\dfrac{R}{R-y} \\ z & -\omega & -z^2 & -z\omega\dfrac{R}{R-y} \\ \omega & -y\omega & -z\omega & -\omega^2\dfrac{R}{R-y} \end{bmatrix} \frac{R}{R-y}\mathrm{d}A\right) \begin{bmatrix} u_\mathrm{C}' - \dfrac{v_\mathrm{C}}{R} \\ v_\mathrm{C}'' + \dfrac{u_\mathrm{C}'}{R} \\ w_\mathrm{C}'' - \dfrac{\alpha}{R} \\ \dfrac{w_\mathrm{C}''}{R} + \alpha'' \end{bmatrix}. \tag{7}$$

In some previous studies, the influence of the curvature in Eq. (7) is completely disregarded, like in [2], or it is considered using complex expressions, as in [8]; in this study, only the linear terms of the Maclaurin series expansion of the terms $R/(R-y)$ and $R^2/(R-y)^2$,

$$\frac{R}{R-y} \cong 1 + \frac{y}{R}, \qquad \left(\frac{R}{R-y}\right)^2 \cong 1 + 2\frac{y}{R}, \tag{8}$$

are retained. With the approximations of the curvature effect defined by Eq. (8), the geometric properties of the curved beams, represented as integrals within round brackets in Eq. (7), can be calculated using geometric properties of the straight thin-walled beams. For doubly symmetric H cross-sections (Fig. 2), non-zero geometric properties are

$$\begin{aligned} A &= \int_A \mathrm{d}A = bt_0 + 2ht_1, \qquad I_z = \int_A y^2 \mathrm{d}A = t_0 b^3/12 + 2ht_1\left(b/2\right)^2, \\ I_y &= \int_A z^2 \mathrm{d}A = 2t_1 h^3/12, \qquad I_\omega = \int_A \omega^2 \mathrm{d}A = t_1 b^2 h^3/24, \end{aligned} \tag{9}$$

while all other geometric properties vanish since $\int_A y\mathrm{d}A = \int_A z\mathrm{d}A = \int_A \omega\mathrm{d}A = \int_A y\omega\mathrm{d}A = \int_A z\omega\mathrm{d}A = \int_A y\omega^2\mathrm{d}A = \int_A y^2\omega\mathrm{d}A = \int_A y^3\mathrm{d}A = 0$. Thus, internal force–displacement relations, Eq. (7), are transformed into a simplified, approximate form

$$\begin{aligned} N &= EA\left(u_\mathrm{C}' - \frac{v_\mathrm{C}}{R}\right) - \frac{EI_z}{R}\left(v_\mathrm{C}'' + \frac{u_\mathrm{C}'}{R}\right) \\ M_z &= EI_z\left(v_\mathrm{C}'' + \frac{v_\mathrm{C}}{R^2}\right) \\ M_y &= -EI_y\left(w_\mathrm{C}'' - \frac{\alpha}{R}\right) - 2\frac{EI_\omega}{R}\left(\frac{w_\mathrm{C}''}{R} + \alpha''\right) \\ B &= -\frac{EI_\omega}{R}\left(w_\mathrm{C}'' - \frac{\alpha}{R}\right) - EI_\omega\left(\frac{w_\mathrm{C}''}{R} + \alpha''\right) \end{aligned}. \tag{10}$$

According to the equations listed in (10), in-plane displacements (u_C and v_C) and in-plane internal forces (N and M_z) are decoupled from out-of-plane displacements (w_C and α) and out-of-plane internal forces (M_y and B) for this type of cross-section. This observation is valid regardless of the terms used to describe the curvature effect. Furthermore, by letting $R \to \infty$ in Eqs. (10), it is easy to verify whether the internal force–displacement relations for the straight thin-walled beams [2] are recovered.

The relationship between the warping moment M_ω and the bimoment B for the straight thin-walled beams [2] is defined as

$$M_\omega = B' . \tag{11}$$

According to [1, 33], Eq. (11) can be applied to curved beams with an I-shaped cross-section, while in the case of H-shaped cross-section, a bimoment given by Eq. (6) must be redefined as

$$B_{c\mathrm{H}} = \int_A \sigma_x \omega \frac{R}{R-y}\mathrm{d}A . \tag{12}$$

Since the analysis presented in this paper is limited to beams with small and moderate initial curvatures, the difference between the - B, Eqs. (6) or (10), and the modified bimoment $B_{c\mathrm{H}}$, (Eq. 12), is neglected to obtain further simplification in this analysis. Then, the total torsional moment M_x can be expressed as follows:

$$M_x = M_\omega + M_t , \tag{13}$$

where the pure torsional moment of a curved beam M_t is expressed as in [1]:

$$M_t = GI_{tc}\left(\alpha' + \frac{w_\mathrm{C}'}{R}\right). \tag{14}$$

In expression (14), G is the shear modulus and I_{tc} is the torsional moment of inertia for a curved thin-walled beam [1], defined as

$$I_{tc} = \frac{1}{3}\int_A \left(\frac{R}{R-y}\right)^2 t^2\mathrm{d}A , \tag{15}$$

where t is the wall thickness.

Using Eqs. (8) and (15), and noting that $\int_A yt^2 \mathrm{d}A = 0$ for this type of cross-section, the following simplification is obtained:

$$I_{tc} \cong \frac{1}{3}\int_A t^2 \mathrm{d}A = I_t = \frac{1}{3}\left(bt_0^3 + 2ht_1^3\right), \tag{16}$$

where I_t represents the torsional moment of inertia for a straight thin-walled beam.

Finally, using Eqs. (5) and (10), the normal stress can be related to the internal forces as follows:

$$\sigma_x = \frac{R}{I_\omega\left(2 - R^2 I_y / I_\omega\right)}\left[\left(2B - M_y R\right)z + \frac{R}{R-y}\left(M_y - BR\, I_y / I_\omega\right)\omega\right]\frac{R}{R-y}. \tag{17}$$

2.3 Equilibrium and governing equations

Since all internal forces for doubly symmetric cross-sections are defined with respect to the cross-section centroid, the infinitesimal segment dx of the curved centroid line with out-of-plane internal forces and distributed line loads is shown in Fig. 3, where $\mathrm{d}x = R\mathrm{d}\phi$, Q_z and q_z are the shear force and the distributed line load in the z-axis direction, respectively, and m_x is the distributed torsional load along the curved centroid line. According to the constraint (b) given in section 2.1, only the constant distributed line loads are considered in this analysis (q_z = const.; m_x = const.).

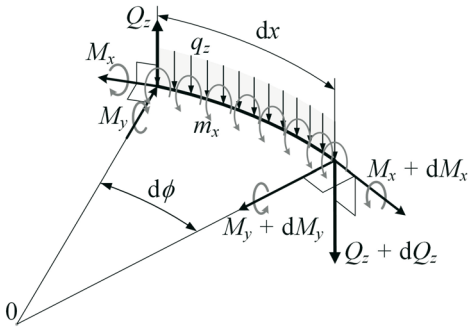

Fig. 3 Infinitesimal segment of a curved centroid line with out-of-plane internal forces and distributed loads

Using Fig. 3, the differential equilibrium equations required for the out-of-plane static analysis are obtained:

$$\begin{aligned} &Q_z' + q_z = 0 \\ &M_x' - \frac{M_y}{R} + m_x = 0 \\ &M_y' - Q_z + \frac{M_x}{R} = 0 \end{aligned}. \tag{18}$$

A detailed explanation of the derivation of the moment equilibrium equations is given in Appendix A. If the shear force Q_z is eliminated from these expressions, the system (18) is reduced to two differential equations:

$$\begin{aligned} &M_x' - \frac{M_y}{R} + m_x = 0 \\ &M_y'' + \frac{M_x'}{R} + q_z = 0 \end{aligned}. \tag{19}$$

Using Eqs. (10), (11), (13), (14), (16), and (19), the governing equations for this approximate approach are derived:

$$\begin{aligned}
&\alpha'''' - \left(3+k^2\right)\frac{\alpha''}{R^2} + n^2\frac{\alpha}{R^4} + 2\frac{w_C''''}{R} - \left(2+n^2+k^2\right)\frac{w_C''}{R^3} - \frac{m_x}{EI_\omega} = 0 \\
&3\alpha'''' - \left(1+n^2+k^2\right)\frac{\alpha''}{R^2} + \left(4+n^2\right)\frac{w_C''''}{R} - k^2\frac{w_C''}{R^3} - \frac{q_z R}{EI_\omega} = 0
\end{aligned} \quad , \tag{20}$$

where $k^2 = R^2 GI_t/(EI_\omega)$ and $n^2 = R^2 I_y/I_\omega$ are the torsional-flexural constants. The solutions of these governing equations can be defined as follows:

$$\begin{aligned}
w_C(\phi) &= C_1 + C_2\phi + D_3\left[C_3\cosh(D_1\phi) + C_4\sinh(D_1\phi)\right] + \\
&\quad + \left(C_5 + C_6 D_2\phi\right)\cos\phi + \left(C_7 + C_8 D_2\phi\right)\sin\phi + R\cdot C_9 - \frac{q_z R^4}{EI_y}\frac{n^2}{k^2}\frac{\phi^2}{2} \\
\alpha(\phi) &= D_4\left[C_3\cosh(D_1\phi) + C_4\sinh(D_1\phi)\right] - \\
&\quad - \frac{1}{R}\left(C_8 R^2 + C_5 + C_6 D_2\phi\right)\cos\phi + \frac{1}{R}\left(C_6 R^2 - C_7 - C_8 D_2\phi\right)\sin\phi - C_9
\end{aligned} \quad , \tag{21}$$

where $\phi = x/R$. In the equations above, $C_1 \ldots C_8$ are integration constants, while C_9 is introduced to simplify a particular solution. With the introduction of $H_1 = 2k^2 - n^2 + 2$ and $H_2 = n^2(k^2+1) - 2$, auxiliary constants $D_1 \ldots D_4$ are defined as

$$\begin{aligned}
D_1 &= \frac{kn}{\sqrt{n^2-2}}, & D_2 &= -\frac{R^2}{2}\frac{k^2+n^2+4}{n^2+1}, \\
D_3 &= \frac{R^2}{D_1}\frac{H_1}{H_2}, & D_4 &= -\frac{R}{D_1}\frac{k^2(n^2+2)}{H_2}.
\end{aligned} \tag{22}$$

In this paper, the integration constants are determined based on the initial parameters arranged into an initial state vector,

$$\mathbf{v}\big|_{x=0} = \mathbf{v}_0 = \left[Q_{z0}\ \ M_{y0}\ \ \beta_0\ \ w_{C0}\ \ M_{x0}\ \ B_0\ \ \vartheta_0\ \ \alpha_0\right]^T. \tag{23}$$

The initial parameters, i.e., the internal forces and displacements at the initial section $x = 0$ are calculated by introducing w_C and α, Eq. (21), into Eqs. (3), (10), (11), and (13). Thus, a system of eight algebraic equations is generated and solved to obtain eight unknown integration constants ($C_1 \ldots C_8$) as functions of the initial parameters from Eq. (23). Introducing $H_3 = k^2n^2(k^2+n^2+1) + 3n^2(n^2-1) - 6$, these integration constants are expressed as follows:

$$\begin{aligned}
C_1 &= w_{C0} + R\alpha_0 + \frac{R}{GI_t}\left[M_{y0}R + B_0 - \frac{q_z R^3}{D_1^2} + \left(q_z R^3 - m_x R^2\right)\left(1 + \frac{1}{n^2}\right)\right] \\
C_2 &= \frac{R^3}{GI_t}Q_{z0} \\
C_3 &= \frac{D_1}{GI_t}\left[-\frac{H_1 - k^2}{H_2}M_{y0} + \frac{B_0}{R} + R\frac{(H_1-k^2)q_z R - k^2(n^2+1)m_x}{D_1^2 H_2}\right] \\
C_4 &= \vartheta_0 + \frac{R^2}{EI_\omega H_2}\left[\left(1 - \frac{H_1}{k^2}\right)Q_{z0}R + (n^2+1)M_{x0}\right]
\end{aligned} \tag{24}$$

$$
\begin{aligned}
C_5 &= -R\alpha_0 + \frac{R^3}{EI_\omega H_2}\left[\left(\frac{H_1 - n^4 + 4}{H_2} - n^2\right)M_{y0}R - (n^2+2)B_0\right] + \\
&\quad + \frac{R^5}{EI_\omega H_2^2}\left\{-q_z R\left[H_3 + 2(H_2 - H_1) + k^2 n^2 (n^2+2)\right] + m_x\left[H_3 + (n^2-2)H_1\right]\right\} \\
C_6 &= \frac{R^2}{EI_\omega}\frac{n^2+1}{H_2}\left(-Q_{z0}R + M_{x0}\right) \\
C_7 &= -R\beta_0 - R^2\frac{H_1}{H_2}\vartheta_0 + \\
&\quad + \frac{R^4}{2EI_\omega H_2^2}\left\{\left[H_3 - 3H_1\right]M_{x0} - \left[2(n^2+2)H_2 + H_3 - 3H_1\right]Q_{z0}R\right\} \\
C_8 &= \frac{R^2}{EI_\omega}\frac{n^2+1}{H_2}\left(M_{y0} + q_z R^2 - m_x R\right) \\
C_9 &= \frac{R^2}{EI_y}\left(q_z R\frac{k^2 + n^2 + 2}{k^2} - m_x\right)
\end{aligned}
\tag{24}
$$

Using the solutions and definitions of the state vector variables according to Eq. (23), the derivation of the field matrix, **K**, and the load vector, **I**, is straightforward and leads to the basic equation of the method of initial parameters,

$$\mathbf{v} = \mathbf{K}\mathbf{v}_0 + \mathbf{I}\,. \tag{25}$$

Since some members of **K** and **I** are too long, they are not presented in the paper.

According to [33], the boundary conditions for the static analysis of thin-walled curved beams can be defined in several ways. In this paper, the boundary conditions for the out-of-plane analysis and different types of supports are adopted according to Table 1.

Table 1 Boundary conditions for the supports of thin-walled curved beams

Clamped end	$w_C = 0$, $\beta = 0$, $\alpha = 0$, $\vartheta = 0$
Simply supported	$w_C = 0$, $M_y = 0$, $\alpha = 0$, $B = 0$
Symmetry	$Q_z = 0$, $\beta = 0$, $M_x = 0$, $\vartheta = 0$

The boundary conditions listed in Table 1 are also valid for Vlasov's approach, whose governing expressions and analytical solutions are given in Appendix B.

3. Illustrative example

In this section, the out-of-plane static analysis of a curved beam clamped at both ends and loaded with a uniformly distributed load q_z at the centroid line of a radius R, as shown in Fig. 4, is performed. The beam length is calculated as $L = R\Phi$, where Φ is the central angle. Using the symmetry, only half of the beam is analysed, as shown in Fig. 5; the symmetry joint with released antisymmetric degrees of freedom (DOFs) in the symmetry plane, i.e. in the mid-span section M, is introduced.

The H-beam analysed in this section has the following geometric (Fig. 2) and material properties: $b = 200$ mm, $h = 100$ mm, and $t = 10$ mm; $E = 73$ GPa and $G = 28$ GPa ($\nu = 0.3036$). For these data, the moments of area are calculated according to Eqs. (9) and (16): $I_t = 13.33 \cdot 10^4$ mm^4, $I_y = 166.67 \cdot 10^4$ mm^4, and $I_\omega = 16666.67 \cdot 10^6$ mm^6.

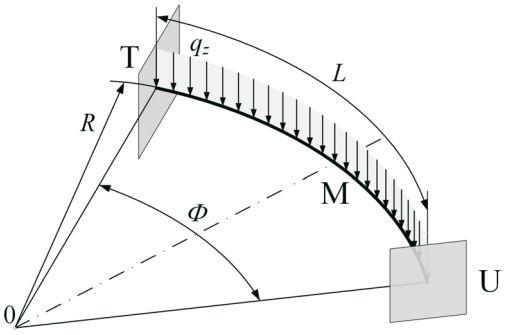

Fig. 4 Complete curved beam model

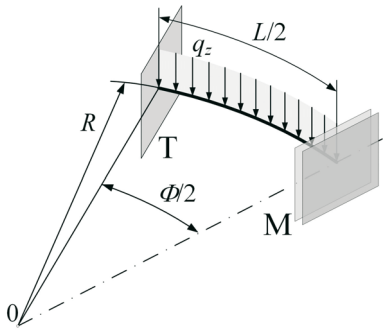

Fig. 5 Symmetric curved beam model

The results obtained using the analytical approach presented in this paper (LC = Linearized Curvature) and Vlasov's approach (VL) are compared with the solutions obtained using the finite element method (FEM). The finite element analysis is performed using ADINA [32], where 4-noded shell finite elements with an average size of 10 mm are used for all beams analyzed. At the clamped end, all DOFs are restrained (thus restraining warping also), while the boundary conditions at the symmetry plane are defined to restrain symmetric displacements only. A cylindrical coordinate system is introduced to define the beam geometry and consequently the local coordinate axes. The constant line load, $q_z = 1$ N/mm, acts along the curved centroid line. The generated finite element mesh with the load and boundary conditions is shown in Fig. 6a. The undeformed (dashed lines) and deformed configurations of the FEM model are shown in Fig. 6b.

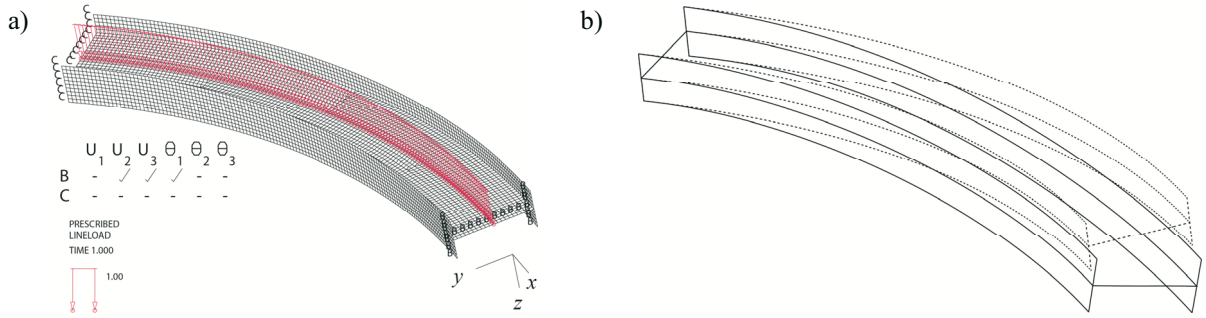

Fig. 6 FEM model of a curved beam with medium curvature, ($R/b = 8$):
a) FEM mesh, boundary conditions, and load; b) undeformed and deformed configurations

The analytical solutions are compared with the numerical ones for various beam lengths L and radii of curvature R, resulting in several hundred processed models. The solutions for the centroid deflections w_C and the angles of torsion α according to (21) are normalised with their absolute maximum values, $\tilde{w} = w_C/|w_C|_{max}$ and $\tilde{\alpha} = \alpha/|\alpha|_{max}$, and shown in Fig. 7 for moderately curved beams ($R/b = 8$). The maximums, $|w_C|_{max}$ and $|\alpha|_{max}$, as absolute values, occur at the beam mid-span, $x/L = 1/2$. The distributions in Fig. 7 are shown along half of the beam length ($0 \le x/L \le 1/2$) for different central angles Φ. Since $L = R\Phi$, the beam length is related to the value of Φ for $R = $ const.; e.g., for $R/b = 8$ and $\Phi = 1$, $L/b = 8$ or for $\Phi = 3$, $L/b = 24$ (corresponding to a very long beam).

Figure 7a shows the normalised w_C distribution, that is almost identical irrespective of the value of Φ. On the other hand, the distribution of the normalised α depends on the value of Φ. For lower Φ values, the normalised α decreases monotonically from zero at the clamped end, with one inflection point. For higher values of Φ, the distributions of the normalised α increase at the beginning and then decrease to the lowest negative value at the symmetry plane, resulting in two inflection points. The distributions of the normalised w_C and α obtained using Vlasov's approach and FEM are identical in shape with the solutions shown in Fig. 7; therefore, they are omitted.

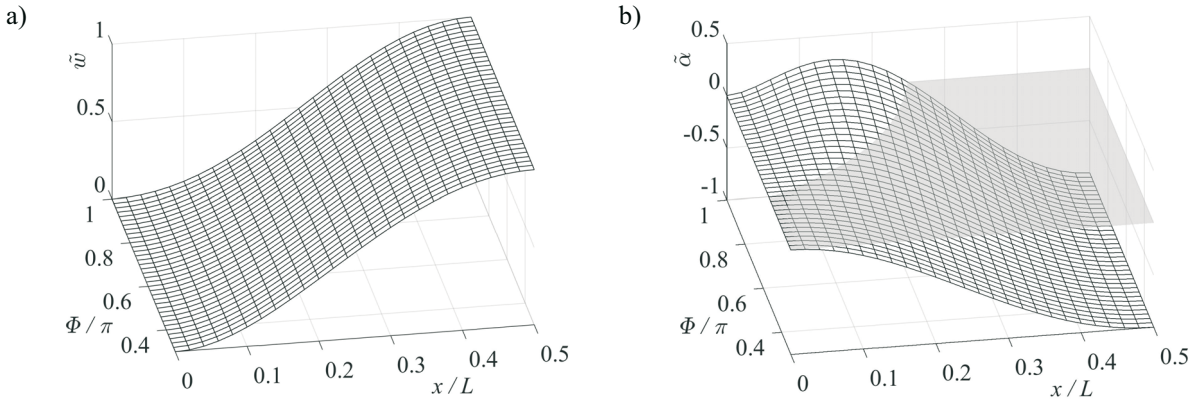

Fig. 7 Analytical LC solutions for R/b = 8:
a) normalised centroid deflections; *b*) normalised angles of torsion

Taking the FEM solutions as reference, the comparison between the LC an VL methods can be established on the basis of relative errors of the solutions calculated at the beam mid-span according to

$$\delta w_{\mathrm{C}}^{\mathrm{LC,VL}} = \frac{w_{\mathrm{C}}^{\mathrm{LC,VL}} - w_{\mathrm{C}}^{\mathrm{FEM}}}{w_{\mathrm{C}}^{\mathrm{FEM}}} \cdot 100, \qquad \delta\alpha^{\mathrm{LC,VL}} = \frac{\alpha^{\mathrm{LC,VL}} - \alpha^{\mathrm{FEM}}}{\alpha^{\mathrm{FEM}}} \cdot 100\,. \tag{26}$$

The relative errors calculated for various curvatures and central angles are shown in Tables 2 and 3.

Table 2 Relative errors of the centroid deflections for the beams with medium curvature at the beam mid-span

	R/b=7			R/b=8			R/b=9			R/b=10		
Φ	$\pi/2$	$3\pi/4$	π	$\pi/2$	$3\pi/4$	π	$\pi/2$	$3\pi/4$	π	$\pi/2$	$3\pi/4$	π
LC	−10.9	−11.7	−12.6	−8.85	−9.49	−10.2	−7.28	−7.78	−8.33	−6.03	−6.45	−6.89
VL	−14.7	−13.7	−13.8	−12.0	−11.0	−11.2	−9.94	−9.12	−9.21	−8.30	−7.59	−7.65

Table 3 Relative errors of the angle of torsion for the beams with medium curvature at the beam mid-span

	R/b=7			R/b=8			R/b=9			R/b=10		
Φ	$\pi/2$	$3\pi/4$	π	$\pi/2$	$3\pi/4$	π	$\pi/2$	$3\pi/4$	π	$\pi/2$	$3\pi/4$	π
LC	−14.3	−14.1	−15.0	−12.1	−12.0	−12.0	−10.2	−9.89	−9.72	−8.69	−8.24	−7.96
VL	−20.3	−17.1	−16.3	−16.8	−13.8	−13.1	−14.0	−11.4	−10.6	−11.8	−9.42	−8.96

From Tables 2 and 3, it is easy to observe that w_{C} and α solutions obtained by the LC method for moderately curved beams are closer to FEM solutions than Vlasov's solutions for all central angles ($\Phi = \pi/2, 3\pi/4, \pi$). The difference between the LC and VL solutions is more pronounced for lower central angles (e.g., $\pi/2$), especially for the solutions of α for all curvatures. For higher central angles (e.g., π), these differences are smaller, and for larger curvatures ($\Phi = \pi$, R/b = 10) are practically negligible. This observation justifies the usage of Vlasov's approach for the determination of displacements for long beams with small and medium curvatures.

The bending moment M_y and the bimoment B calculated according to (10) and (21) are normalised with respect to their absolute maximum values, ($\tilde{M}_y = M/|M_y|_{\max}$ and $\tilde{B} = B/|B|_{\max}$), and shown in Fig. 8 for a constant beam length of L/b = 10 and different curvatures.

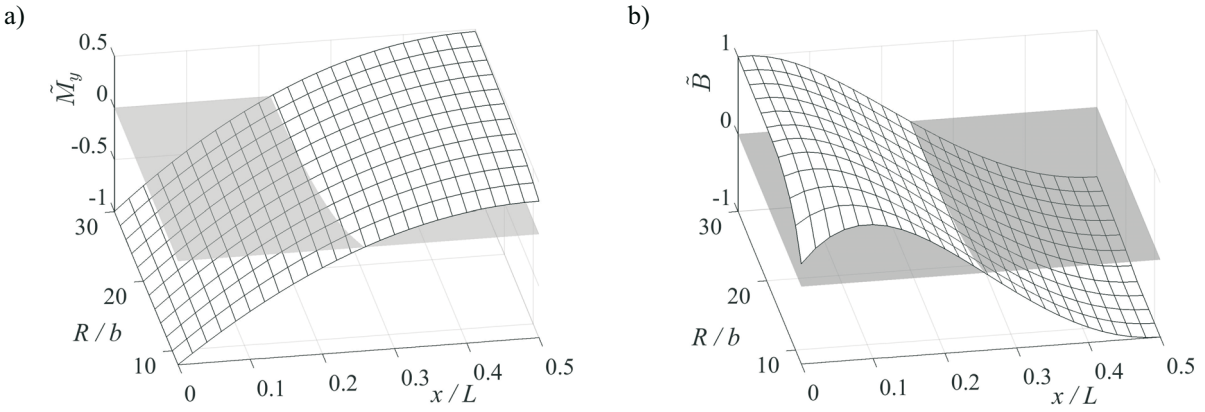

Fig. 8 The normalised distributions obtained by the LC method for beams with $L/b = 10$: *a*) bending moment; *b*) bimoment

Due to the uniformly distributed load, the normalised distribution of M_y along the half of the beam length (Fig. 8a) is similar to the analogous distribution of M_y for straight beams regardless of the beam curvatures. The largest bending moment occurs at the clamped end, and about half of its value occurs at the beam mid-span; the unfolded (longitudinal) distribution for curved beams is very similar to quadratic distribution. From Fig. 8b, one can see that the normalised B distribution depends on the curvature. For medium curvatures ($R/b < 10$), the normalised B distribution first increases and then decreases, showing two inflection points. For larger curvatures ($R/b > 10$), the normalised B distribution monotonically decreases with one inflection point similar to the distribution of bimoment for straight beams.

Regarding the normal stress distribution along the cross-section contour, it should be emphasized that, for this type of cross-section, the normal stress at the horizontal wall (line FCG in Fig. 2) is zero. The normal stress along vertical cross-section walls (lines AFD and BGE in Fig. 2) is linearly distributed with different extreme values at the wall end points A and B (or D and E). The distributions of normal stresses along the inner (point A) and outer (point B) flanges for a moderately curved beam with $R/b = 8$ and central angle $\Phi = 2\pi/5$ (i.e., $L/b = 10.1$) are shown in Fig. 9a, and the distributions for $\Phi = \pi$ (i.e., $L/b = 25.1$) in Fig. 9b.

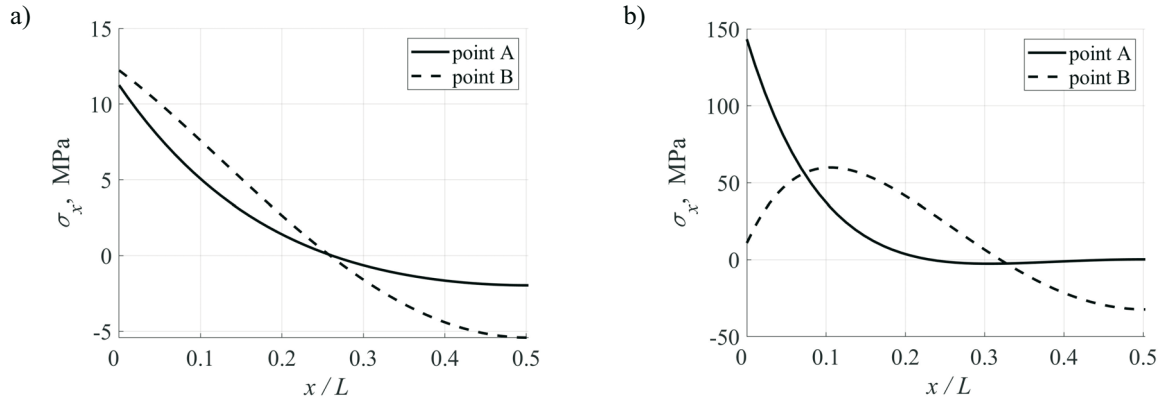

Fig. 9 The longitudinal distributions of the normal stress obtained by the LC method at the inner (point A) and the outer (point B) flange for $R/b = 8$ and for: *a*) $\Phi = 2\pi/5$; *b*) $\Phi = \pi$

For the beam with $R/b = 8$ and $\Phi = 2\pi/5$, the maximum normal stress occurs at the clamped end ($x = 0$) at point B of the outer flange. This value is slightly higher but very close to the stress value at point A of the inner flange at the same section, Fig. 9a. While approaching the beam mid-span, the normal stresses on both flanges decrease, but with

different gradients. At the beam mid-span, the normal stress is much higher at the outer flange than at the inner flange, as can be seen from Fig. 9a. For longer beams, the maximum value of normal stress occurs at the inner flange of the clamped end, which is shown in Fig. 9b. On the beam in this figure, three different regions can be distinguished: i) a region near the clamped end where stresses at the inner flange are dominant; ii) a region where stresses at the outer flange are dominant; and iii) a region where stresses at the inner flange approach zero while stresses at the outer flange decrease monotonically to the minimum at the plane of symmetry ($x/L = 1/2$). The value of the maximum stress $\sigma_{x,\max}$ at the outer flange (point B) and its position $x_{\max}$ for the distribution in Fig. 9b, calculated using the LC, VL, and FEM methods, are presented in Table 4.

Table 4 Position and value of the maximum normal stress at the outer flange for $R/b = 8$ and $\Phi = \pi$

	FEM	LC	VL
$x_{\max}$ (mm)	527.1	527.7	512.0
$\sigma_{x,\max}$ (MPa)	56.8	59.8	62.4

Analysing the results shown in Table 4, it is obvious that the LC method predicts the FEM solution more accurately than the VL method, again.

Figure 10 shows the normal stresses calculated for various R/b and Φ for point A at the clamped end.

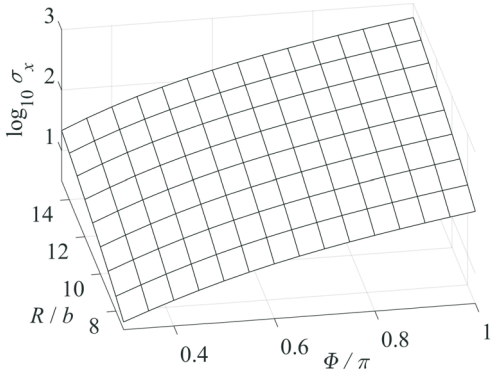

Fig. 10 The normal stress obtained by the LC method for point *A* at the clamped end

In this figure, the curvatures, R/b, and the central angles, Φ, are shown in a linear scale, while the stress, σ_x^{LC}, expressed in MPa, is given in a logarithmic scale. As expected, the normal stress at point A of the clamped end increases with the increasing values of the centroid line radius R and the beam length L. Figure 10 can be also used to determine the value of normal stress for any combination of curvatures, central angles, and distributed load values since the results shown were obtained for $q_z = 1$ N/mm.

A better comparison of analytical methods can be drawn by calculating the relative errors of normal stresses with respect to the FEM stress according to

$$\delta\sigma_x^{\mathrm{LC,VL}} = \frac{\sigma_x^{\mathrm{LC,VL}} - \sigma_x^{\mathrm{FEM}}}{\sigma_x^{\mathrm{FEM}}} \cdot 100 \,. \tag{27}$$

Using the above expression, the relative errors of normal stresses obtained by both analytical methods for moderately curved beams and various central angles at flange edges A and B are shown in Tables 5 and 6. These stresses are calculated at the position $x/b = 1$ along the centroid line in order to avoid numerical difficulties of the FEM solution at the clamped end.

Table 5 Relative normal stress errors for moderately curved beams at point A of the inner flange and for $x = b$

	R/b=7			R/b=8			R/b=9			R/b=10		
Φ	$\pi/2$	$3\pi/4$	π	$\pi/2$	$3\pi/4$	π	$\pi/2$	$3\pi/4$	π	$\pi/2$	$3\pi/4$	π
LC	−7.52	−2.84	−0.67	−5.52	−2.05	−0.21	−4.19	−1.46	+0.11	−3.25	−1.03	+0.31
VL	−16.1	−10.2	−6.85	−12.9	−8.26	−5.36	−10.6	−6.79	−4.27	−8.93	−5.67	−3.48

Table 6 Relative normal stress errors for moderately curved beams at point B of the outer flange and for $x = b$

	R/b=7			R/b=8			R/b=9			R/b=10		
Φ	$\pi/2$	$3\pi/4$	π	$\pi/2$	$3\pi/4$	π	$\pi/2$	$3\pi/4$	π	$\pi/2$	$3\pi/4$	π
LC	5.47	5.78	7.16	4.28	5.01	6.26	3.54	4.42	5.57	3.04	3.96	5.12
VL	8.33	12.0	16.9	7.31	11.0	15.7	6.63	10.1	14.9	6.13	9.45	14.3

Comparing the results of the two methods, it is obvious that the proposed LC method gives a better prediction of the FEM normal stresses than Vlasov's method. This difference is more evident here than in the case of the displacement comparison. For both flanges (points A and B), the stress relative error decreases with the increasing curvature for moderately curved beams ($7 \le R/b \le 10$). According to Tables 5 and 6, the value of the central angle, Φ, i.e., the beam length L, affects the stress relative error at the inner and outer flanges differently. For the inner flange (Table 5), and for all curvatures, the stress relative errors decrease for higher values of Φ in both analytical methods. The stress relative errors determined with the LC method are significantly smaller than those determined with Vlasov's method. For the outer flange (Table 6), this trend is reversed, i.e., the increase in the value of Φ increases the relative error, but for higher Φ values, the LC method predicts the FEM stresses better. This trend is maintained even for slightly curved beams with $R/b > 10$ when a small increase in the value of relative error is observed for point B of the outer flange, as it is shown in Table 7.

Table 7 Relative normal stress errors for slightly curved beams at point B of the outer flange for $x = b$ and $\Phi = \pi$

R/b	11	12	13	14	15
LC	4.75	4.75	4.79	5.00	5.30
VL	14.0	14.0	14.1	14.5	14.9

From Table 7, which shows the solutions for $\Phi = \pi$ and slightly curved beams ($11 \le R/b \le 15$), it is easy to conclude that an increase in the value of the radius of curvature has no significant effect on the relative normal stress errors at the outer flange, but the LC solutions are still considerably closer to the FEM solutions.

4. Conclusions

A comprehensive analytical approach for the determination of displacements and normal stresses of moderately and slightly curved thin-walled beams with doubly symmetric H cross-section is presented. Only the uniformly distributed out-of-plane loads are considered. By neglecting the higher order terms of the Maclaurin series expansion, the terms containing the curvature effect in expressions for internal forces are linearized. These terms are neglected in Vlasov's approach for the analysis of thin-walled curved beams, making it primarily intended for the analysis of beams with small curvature. The linearization of the terms related to the curvature extends the capability of this approach to the analysis of moderately curved beams. Moreover, this linearization allows the use of geometric properties of the straight thin-walled beam in the analysis of the curved beams without modifications. A further simplification results from the use of warping moment–bimoment (M_ω–B) relation for the straight thin-walled beams in the presented approach, thus avoiding the introduction of the modified bimoment as in

[1, 33]. The proposed method and Vlasov's method, as a fundamental and one of the earliest models for the analysis of the thin-walled beams, are compared by calculating displacements and normal stress relative errors with respect to the numerical solution obtained using shell finite elements. The influence of the curvature effect and the beam length is investigated using the R/b ratio and the central angle, Φ. It is shown that both approaches approximate the finite element solution for centroid line deflections in a similar way. The proposed approach gives a better approximation of the twist angles than Vlasov's approach for moderately curved beams, especially for smaller beam central angles. Even better results are obtained for the normal stress distribution as the dominant stress component. The proposed method provides the solutions 2-6 times closer to the finite element solutions than Vlasov's solutions, for small and medium curvatures and for the inner and outer flanges irrespective of the beam central angle. These results justify the use of the proposed closed-form approximate solutions in the analysis of long, slightly and moderately curved thin-walled beams, especially in the early design stages when a large number of analyses can be performed efficiently.

Based on the extensive research conducted in the preparation of this paper, it should be noted that none of the approaches presented in [1-17], including the approach presented in this paper, are suitable for the analysis of short and relatively short thin-walled curved beams. The values of displacements and stress relative errors calculated by the previously mentioned methods are rather high for the moderately curved beams with $L/b < 8$. Also, based on the authors' experience in the analysis of the straight thin-walled beams, this observation leads to the conclusion that the shear stress in the middle surface cannot be neglected in the analysis of relatively short thin-walled curved beams, as it is assumed in the introduction of the paper. The influence of shear taken into account with approximate analytical expressions is well investigated in the analysis of the straight thin-walled beams [35-37]. As for curved thin-walled beams, the number of references related to the analytical solutions for this subject is very limited. To the authors' knowledge, only Kano et al [38] included the influence of shear in the analysis of thin-walled curved beams by the method of successive approximations over equilibrium conditions for the infinitesimal wall element. Our further research into the thin-walled curved beam will include the analysis of other doubly symmetric cross-sections, different load types and boundary conditions, and the application of this approach to the curved composite thin-walled beams.

REFERENCES

[1] Tong, G.; Xu, Q.: "An Exact Theory for Curved Beams with Any Thin-Walled Open Sections", Advances in Structural Engineering, Vol. 5, No. 4, pp. 195 -209, 2002. https://doi.org/10.1260/136943302320974572

[2] Vlasov, V. Z.: "Thin-Walled Elastic Beams, Second Edition", Israel Program for Scientific Translations, Jeruzalem, 1963.

[3] Timoshenko, S. P.; Gere, J. M.: "Theory of elastic stability (2nd ed.)", McGraw-Hill, 1961.

[4] Yoo, C.H.: "Flexural-torsional stability of curved beams", Journal of the Engineering Mechanics Division, Vol. 108, No. 6, pp. 1351-1369, 1982. https://doi.org/10.1061/JMCEA3.0002908

[5] Nishino, F.; Fukasawa, Y.: "Formulation of static behavior of thin-walled curved beams under assumptions of strain field", Proceedings of the Japan Society of Civil Engineers, Vol. 1976, No. 247, pp. 9-19, 1976. https://doi.org/10.2208/jscej1969.1976.247_9

[6] Usami, T.; Koh, S.Y.: "Large displacement theory of thin-walled curved members and its application to lateral-torsional buckling analysis of circular arches", International Journal of Solids and Structures, Vol. 16, No. 1, pp. 71-95, 1980. https://doi.org/10.1016/0020-7683(80)90096-7

[7] Kang Y.J., Yoo C.H., Thin-walled curved beams. I: Formulation of nonlinear equations, J. Eng. Mech. 120: 2072-2101, 1994. https://doi.org/10.1061/(ASCE)0733-9399(1994)120:10(2072)

[8] Kim, N. I.; Kim, M. Y.: "Thin-walled curved beam theory based on centroid-shear center formulation", Journal of Mechanical Science and Technology, Vol. 19, No. 2, pp. 589-604, 2005. https://doi.org/10.1007/BF02916181

[9] Yang, Y.; Kuo, S.: "Static Stability of Curved Thin-Walled Beams", Journal of Engineering Mechanics, Vol. 112, No. 8, pp. 821-841, 1986. https://doi.org/10.1061/(ASCE)0733-9399(1986)112:8(821)

[10] Yang Y.; Kuo S.: "Effect of curvature on stability of curved beams", Journal of Structural Engineering, Vol. 113, pp. 1185-1202, 1987. https://doi.org/10.1061/(ASCE)0733-9445(1987)113:6(1185)

[11] Yang, Y., Kuo, S., Cherng, Y.: "Curved Beam Elements for Nonlinear Analysis", Journal of Engineering Mechanics, Vol. 115, No. 4, pp. 840-855, 1989. https://doi.org/10.1061/(ASCE)0733-9399(1989)115:4(840)

[12] Kang, Y.J.; Yoo, C.H.: "Thin-walled curved beams. II: Analytical Solutions for Buckling of Arches", Journal of Engineering Mechanics, Vol. 120, No. 10, pp. 2102-2125, 1994. https://doi.org/10.1061/(ASCE)0733-9399(1994)120:10(2102)

[13] Flüge W., Stresses in Shells, Springer-Verlag, Berlin, 1973. https://doi.org/10.1007/978-3-642-88291-3

[14] Zeybek, Z.; Topkaya, C.; Rotter, J. M.: "Analysis of silo supporting ring beams resting on discrete supports", Thin-Walled Structures, Vol. 135, pp. 285-296, 2019. https://doi.org/10.1016/j.tws.2018.11.001

[15] Zeybek, Z.; Seçer, M.: "A design approach for the ring girder in elevated steel silos", Thin-Walled Structures, Vol. 157, 2020. https://doi.org/10.1016/j.tws.2020.107002

[16] Huang, S.; Qiao, P.:"Buckling of thin-walled I-section laminated composite curved beams", Thin-Walled Structures, Vol. 154, p. 106843, 2020. https://doi.org/10.1016/j.tws.2020.106843

[17] Kustura D.; Vlak F.; Matić T.; Vukasović M.: "In-plane Displacements of Thin-walled Curved Beams", 2022 7th International Conference on Smart and Sustainable Technologies (SpliTech), Split / Bol, Croatia, 2022, pp. 1-5. https://doi.org/10.23919/SpliTech55088.2022.9854356

[18] Kvaternik, S.; Turkalj, G.; Lanc, D.: "Analysis of flexure, torsion and buckling of thin-walled frames with a focus on the joint warping behaviour ", Transactions of FAMENA, Vol. 41, No. 4, pp. 1-10, 2017. https://doi.org/10.21278/TOF.41401

[19] Ribarić, D: "A Simple and Efficient Three-Node Curved Beam Element for the Out-of-Plane Shear, Bending and Torsion, Based on the Linked Interpolation Concept ", Transactions of FAMENA, Vol.45, No. 2, pp. 13-29, 2021. https://doi.org/10.21278/TOF.452023720

[20] Kim, N. I.; Jeon, C. K.: "Improved Thin-Walled Finite Curved Beam Elements", Advances in Mechanical Engineering, Vol. 5, 2013. https://doi.org/10.1155/2013/429658

[21] Piovan, M. T.; Cortínez, V. H.: "Mechanics of thin-walled curved beams made of composite materials, allowing for shear deformability", Thin-Walled Structures, Vol. 45, No. 9, pp. 759-789, 2007. https://doi.org/10.1016/j.tws.2007.06.005

[22] Lezgy-Nazargah, M.: "A finite element model for static analysis of curved thin-walled beams based on the concept of equivalent layered composite cross section", Mechanics of Advanced Materials and Structures, pp. 1-14, 2020. https://doi.org/10.1080/15376494.2020.1804649

[23] Milić, P.; Marinković, D.: "Isogeometric FE analysis of complex thin-walled structures", Transactions of FAMENA, Vol. 39, No. 1, pp. 15-26, 2015.

[24] Tsiptsis, I. N.; Sapountzakis, E. J.: "Generalized warping and distortional analysis of curved beams with isogeometric methods", Computers & Structures, Vol. 191, pp. 33-50, 2017. https://doi.org/10.1016/j.compstruc.2017.06.007

[25] Cazzani, A. et al.: "Constitutive models for strongly curved beams in the frame of isogeometric analysis", Mathematics and Mechanics of Solids, Vol. 21, No. 2, pp. 182-209, 2015. https://doi.org/10.1177/1081286515577043

[26] Cazzani, A.; Malagù M.; Camotim D.: "Isogeometric analysis of plane-curved beams", Mathematics and Mechanics of Solids, Vol. 21, No. 5, pp. 562-577, 2016. https://doi.org/10.1177/1081286514531265

[27] Cárdenas, D. et al.: "Unified theory for curved composite thin-walled beams and its isogeometrical analysis", Thin-Walled Structures, Vol. 131, pp. 838-854, 2018. https://doi.org/10.1016/j.tws.2018.07.036

[28] Nuno, P.: "Formulação linear da Teoria Generalizada de Vigas para barras de eixo curvo", Master's thesis, A Faculdade de Ciências e Tecnologia, Universidade Nova de Lisboa, 2015.

[29] Peres, N.; Gonçalves R.; Turco E.: "First-order generalised beam theory for curved thin-walled members with circular axis", Thin-Walled Structures, Vol. 107, pp. 345-361, 2016. https://doi.org/10.1016/j.tws.2016.06.016

[30] Peres, N.; Gonçalves R.; Camotim D.: "GBT-based cross-section deformation modes for curved thin-walled members with circular axis", Thin-Walled Structures, Vol. 127, pp. 769-780, 2018. https://doi.org/10.1016/j.tws.2018.03.008

[31] Carrera, E.; Giunta, G.; Petrolo, M.: "Beam Structures: Classical and Advanced Theories", Wiley, 2011. https://doi.org/10.1002/9781119978565

[32] De Pietro, G. et al.: "Strong and weak form solutions of curved beams via Carrera's unified formulation", Mechanics of Advanced Materials and Structures, Vol. 27, No. 15, pp. 1342-1353, 2018. https://doi.org/10.1080/15376494.2018.1510066

[33] Tong, G.: "The linear and nonlinear theory of thin-walled curved beams" (Chinese Edition): 薄壁曲梁线性和非线性分析理论", Science Press, 2004.

[34] ADINA 9.3.3. Theory and Modeling Guide, ADINA R&D Inc, Watertown, 2017.

[35] Pavazza, P.; Matoković, A.; Plazibat, B.: "Bending of thin-walled beams of symmetrical open cross-sections with influence of shear", Transactions of Famena, Vol. 37, No. 3, pp. 17-30. 2013.

[36] Pavazza, P.; Matoković, A.; Plazibat, B.: "Torsion of thin-walled beams of symmetrical open cross-sections with influence of shear", Transactions of Famena, Vol. 37, No. 2, pp. 1-14, 2013.

[37] El Fatmi, R.: "Non-uniform warping including the effect of torsion and shear forces. Part I: A general beam theory", International Journal of Solids and Structures, Vol. 44, pp. 5912-5929, 2007. https://doi.org/10.1016/j.ijsolstr.2007.02.006

[38] Kano, T.; Usuki, S.; Hasebe, K.: "Theory of thin-walled curved members with shear deformation", Ingenieur-Archiv, Vol. 51, No. 5, pp. 325-336, 1982. https://doi.org/10.1007/BF00536658

Appendix A

The moment equilibrium equations at the left end section of infinitesimal segment of a curved centroid line shown in Fig. 3 are:

$$\begin{aligned}\sum M_{Ox} &= -M_x + (M_x + \mathrm{d}M_x)\cos\mathrm{d}\phi - (M_y + \mathrm{d}M_y)\sin\mathrm{d}\phi + m_x R\mathrm{d}\phi\cos(\mathrm{d}\phi/2) = 0\\ \sum M_{Oy} &= -M_y + (M_y + \mathrm{d}M_y)\cos\mathrm{d}\phi + (M_x + \mathrm{d}M_x)\sin\mathrm{d}\phi - (Q_z + \mathrm{d}Q_z)R\sin\mathrm{d}\phi = 0\end{aligned}. \quad (A.1)$$

Using $\sin(\mathrm{d}\phi) \approx \mathrm{d}\phi$, $\cos(\mathrm{d}\phi) \approx 1$, $\cos(\mathrm{d}\phi/2) \approx 1$, and after neglecting higher order terms, the previous expressions are transformed into

$$\mathrm{d}M_x - M_y\mathrm{d}\phi + m_x R\mathrm{d}\phi = 0, \qquad \mathrm{d}M_y + M_x\mathrm{d}\phi - Q_z R\mathrm{d}\phi = 0\,. \quad (A.2)$$

With $()' = \mathrm{d}()/\mathrm{d}x$ and $\phi = x/R$, the final form of the moment equilibrium equations given in Eq. (18) is obtained by dividing (A.2) by $R\mathrm{d}\phi$.

Appendix B

Neglecting the curvature effect, i.e., using $R/(R-y) \approx 1$ and $R^2/(R-y)^2 \approx 1$, Vlasov's internal force–displacement relations are recovered from Eqs. (7) and (9) as

$$\begin{aligned} N &= EA\left(u_C' - v_C/R\right), & M_z &= EI_z\left(v_C'' + v_C/R^2\right)\\ M_y &= -EI_y\left(w_C'' - \alpha/R\right), & B &= -EI_\omega\left(w_C''/R + \alpha''\right)\end{aligned}. \quad (B.1)$$

The normal stress according to Vlasov reads

$$\sigma_x = M_y/I_y \cdot z + B/I_\omega \cdot \omega\,. \quad (B.2)$$

Following the procedure described in section 2, and using $k^2 = R^2 GI_t/(EI_\omega)$ and $n^2 = R^2 I_y/I_\omega$, the governing equations according to Vlasov's approach are obtained:

$$\begin{aligned}&\alpha'''' - k^2\frac{\alpha''}{R^2} + n^2\frac{\alpha}{R^4} + \frac{w_C''''}{R} - \left(n^2+k^2\right)\frac{w_C''}{R^3} - \frac{m_x}{EI_\omega} = 0\\ &\alpha'''' - \left(n^2+k^2\right)\frac{\alpha''}{R^2} + \left(1+n^2\right)\frac{w_C''''}{R} - k^2\frac{w_C''}{R^3} - \frac{q_z R}{EI_\omega} = 0\end{aligned}. \quad (B.3)$$

The solutions of these equations are given by Eq. (21) with the following auxiliary constants, $D_1 \ldots D_4$:

$$D_1 = k, \qquad D_2 = -\frac{R^2}{2}\frac{k^2+n^2+1}{n^2}, \qquad D_3 = -\frac{R^2}{k(k^2+1)}, \qquad D_4 = -\frac{Rk}{k^2+1}. \tag{B.4}$$

The unknown integration constants $C_1 \ldots C_9$ are:

$$\begin{aligned}
C_1 &= w_{C0} + R\alpha_0 + \frac{R}{GI_t}\left(M_{y0}R + B_0 - m_x R^2 - q_z R^3 \frac{1-k^2}{k^2} \right) \\
C_2 &= \frac{R^3}{GI_t} Q_{z0} \\
C_3 &= \frac{R}{EI_\omega}\frac{1}{k\left(k^2+1\right)}\left[\left(k^2+1\right)B_0 + M_{y0}R - \frac{q_z R^3}{k^2} - m_x R^2 \right] \\
C_4 &= \vartheta_0 + \frac{R^2}{EI_\omega}\frac{1}{1+k^2}\left(\frac{1}{k^2} Q_{z0}R + M_{x0} \right) \\
C_5 &= -R\alpha_0 - \frac{R^3}{EI_\omega}\left(\frac{k^2+2}{(k^2+1)^2} M_{y0}R + \frac{B_0}{k^2+1} \right) + \\
&\quad \frac{R^3}{EI_y}\left[m_x\left(1 + \frac{n^2(2k^2+3)}{(k^2+1)^2} - \frac{n^2}{k^2+1} \right) - q_z R\left(1 + \frac{n^2(k^2+2)}{(k^2+1)^2} + \frac{n^2}{k^2+1} \right) \right] \\
C_6 &= \frac{R^2}{EI_\omega}\frac{1}{k^2+1}\left(-Q_{z0}R + M_{x0} \right) \\
C_7 &= -R\beta_0 + \frac{R^2}{k^2+1}\vartheta_0 - \frac{R^2}{2EI_y}\left[\left(1 + \frac{3n^2}{k^2+1} + \frac{2n^2}{\left(k^2+1\right)^2} \right) Q_{z0}R - \right. \\
&\quad \left. - \left(1 + \frac{n^2}{k^2+1} + \frac{2n^2}{\left(k^2+1\right)^2} \right) M_{x0} \right] \\
C_8 &= \frac{R^2}{EI_\omega}\frac{1}{1+k^2}\left(M_{y0} + q_z R^2 - m_x R \right) \\
C_9 &= \frac{R^2}{EI_y}\left(q_z R\frac{k^2+n^2}{k^2} - m_x \right)
\end{aligned} \tag{B.5}$$

Submitted: 25.4.2023
Accepted: 09.6.2023

Dražen Kustura
Tomislav Matić
University of Split, Faculty of Science, Ruđera Boškovića 33, 21000 Split, Croatia
Frane Vlak*
Marko Vukasović
University of Split, Faculty of Electrical Engineering, Mechanical Engineering and Naval Architecture, Ruđera Boškovića 32, 21000 Split, Croatia
*Corresponding author:
fvlak@fesb.hr